MASTER THESIS

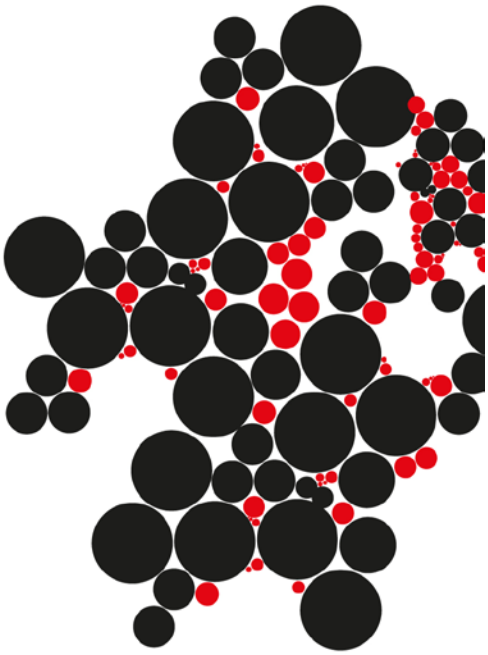

# SELF-ASSEMBLY OF SILICON PARTICLES USING MAGNETIC LEVITATION


Auke J. Been
S0137049

FACULTY OF ELECTRICAL ENGINEERING, MATHEMATICS AND COMPUTER SCIENCE
TRANSDUCERS SCIENCE AND TECHNOLOGY GROUP


EXAMINATION COMMITTEE
Dr.ing. Léon A. Woldering
Prof.dr.ir. Leon Abelmann
Prof.dr. Miko C. Elwenspoek
Prof.dr. Jan C.T. Eijkel

UNIVERSITY OF TWENTE.

11 NOVEMBER 2013

To my parents

# Self-Assembly of Silicon Particles using Magnetic Levitation

Auke Been

11 November 2013

**In this work, self-assembly of cubic silicon particles into a crystalline formation using magnetic levitation is presented. A self-assembly set-up was created and characterised. Template-free self-assembly of hydrophilic particles is compared against (1) template-free self-assembly of hydrophobic particles and (2) templated self-assembly of hydrophilic particles. The results show that (1) hydrophobic functionalisation up to a certain hydrophobicity increases the quality of a self-assembled agglomerate and (2) templated self-assembly increases the amount of good contacts by a factor two compared to template-free self-assembly. The ultimate goal is full three-dimensional microfabrication capabilities.**

## I. Introduction

Microfabrication has had a tremendous impact on technological development. Products enabled by microfabrication technology (computers, internet) have been at the basis of substantial changes in society. Current microfabrication is however limited to layered two-dimensional structures [1]. The limits of the technology are being pushed further and further [2], but eventually the urgency to fully use the third dimension will need to be adressed [3].

One suggested approach of reaching full three-dimensional micromachining capabilities, is through self-assembly [4]. In self-assembly, structured particles are introduced in some kind of environment, where they—under the influence of binding forces and driving forces—form a structured array [5]. An example is a bubble raft of uniform bubbles on the surface of soapy water [6, 7], where a bubble is a particle, the soapy water in a container is the environment, the binding forces are capillary forces and driving forces are mechanical vibrations; when all four elements are brought together, the bubbles form a two-dimensional crystaline structure.

Through self-assembly new systems and materials come into view. Examples are three-dimensional electronics [8, 9], conformal and reconfigurable devices [10], and photonic band-gap materials [11, 12, 13]. In addition, approaches to enhance current fabrication techniques become available, such as further miniaturisation where current industrial robots are unable to assemble smaller parts [14], or assembling components created through a bottom-up approach in nanoscience [14].

Another big advantage of self-assembly in microfabrication is the ability to process components on different wafers, such that each component can be fabricated in the most efficient way [15]. Currently, a complete device is created on one wafer, where a lot of processing steps are needed to protect some elements of the device from processing steps needed for other elements. Separating components onto different wafers, followed by self-assembly will lead to cheaper, more versatile fabrication [15].

Self-assembly in two dimensions has already been thoroughly studied. Examples relevant to this work include (1) the investigation of crystal structures in a bubble raft, as mentioned above [6, 7]. (2) Two-dimensional self-assembly using hydrophobic and hydrophilic interaction between particles on the surface of water [16, 17, 18], where hexagonal particles with functionalised sides form structures through capillary action. Depending on the hydrophobicity/hydrophilicity of the different sides, a variety of structures is formed. (3) Other studies use capillary action to bind loose particles on a substrate with specific binding sites [19, 20, 21, 22].

It appears that capillary action using hydrophobic and hydrophilic interaction is one of the key binding forces used in the current research on self-assembly of mm- and µm-scale particles. That capillary action is not necessary for self-assembly at these scales per se, was shown by etching potential wells in silica [23]. Adding µm-sized spherical particles on the substrate, creates crystal structures in the potential wells much like the bubble rafts.

Capillary forces have also been used in three-dimensional self-assembly: For example mm-scale three-dimensional electronics have been made through

self-assembly. Functionalised cubes were self-assembled through capillary forces of solder in a heated KBr solution [8]. A different approach for three-dimensional self-assembly is to use hydrophilic-hydrophobic interactions between particles. In one publication, silver nanocubes were functionalised to be hydrophobic and allowed to self-assemble, resulting in a lattice of silver nanocubes [24]. Similar results have been obtained for particles of different shapes [25]. Furthermore, a two-step self-assembly process has been reported using a hydrophobic self-assembled monolayer on gold as a first step for self-assembly [26]. In the second step, the pH of the medium was reduced to two, which makes silica become hydrophobic. This controllable hydrophobicity was used for a two-step self-assembly process, and is an interesting control parameter for future projects.

Adding magnetic levitation to three-dimensional self-assembly adds interesting features to the self-assembly process. Advantages of magnetic levitation include (1) prevention of sedimentation of the particles and (2) a controllable force pushing the particles towards each other [27]. (3) Additionally, we foresee that the controllable levitation height adds a potential templating mechanism. One could for example envision layer-by-layer stacking of particles on a template.

Levitating materials with a high diamagnetic constant is straightforward [28]. However, magnetic levitation of materials with a low diamagnetic constant is more challenging, but can be achieved by placing them in a paramagnetic liquid [29]. In such a set-up, the paramagnetic medium will be attracted to the magnets, pushing the diamagnetic material away from the magnets. In this way, magnetic levitation is achieved [30]. Magnetic levitation has already been used for density based separation of materials [29, 31, 32], as well as density measurements and density based chemical reaction detection [33, 34].

Self-assembly and magnetic levitation have been combined in some studies [27, 35]. The magnetic force pushing particles towards the centre axis of the magnets resembles the potential wells etched in silicon mentioned before [23]. Likewise, two-dimensional ordering of particles can be expected in magnetic levitation. Indeed, this phenomenon was reported along with templated self-assembly in two dimensions [27]. In addition, three-dimensional self-assembly using density based separation has been reported [35]. Structured particles of different densities were levitated at different heights in the magnetic set-up. When the paramagnetic medium is drained from the container, a three-dimensional structure remains.

To the best of our knowledge, there are no reports on three-dimensional self-assembly of crystal structures of levitated, non-spherical particles. We believe that self-assembly of non-spherical particles is essential in the roadmap to self-assembled micromachines, which are in essence an assembly of smaller parts of arbitrary shape and size. Gaining knowledge on how these parts can be self-assembled is crucial.

In this work, large cubic particles with edges of 0.5 mm were used. We have chosen for cubic particles, to move away from point symmetry. For spherical particles, the rotation with respect to eachother is not of importance for a perfectly aligned assembly. For square particles, rotation of particles with respect to eachother plays an important role. We believe that understanding self-assembly of square particles, is a first step towards self-assembly with particles of arbitrary shape and size. Silicon was chosen as material because silicon microfabrication is a well established technology. Furthermore, other shapes of silicon particles have been demonstrated [36]. The mm-scale was chosen for simple fabrication and uncomplicated visualisation of the particles. In subsequent research, the system should be miniaturised. Two key elements of this work have been shown to work on smaller scales: (1) Three-dimensional self-assembly using smaller particles has already been achieved [25, 24] and (2) small magnets have been used to magnetically trap particles [37]. Based on the results described in these two articles, we are confident that a future exploration on smaller length scales is feasible.

In this work we will combine self-assembly using magnetic levitation, as pioneered by Illievski [27], with hydrophobic particle interactions [24] to create crystalline three-dimensional macro-structures: Ideally, a cube of 3x3x3 particles will be self-assembled. The self-assembly experiments in this work will be presented along the four key components of self-assembly, as described by Pelesko [5]. (1) Cubic particles of silicon, with a native oxide surface layer, will be used as structured particles. The particles will be functionalised to study the effect of hydrophobic interaction between particles on the self-assembly process. (2) The magnetic field and paramagnetic medium will represent the environment needed for self-assembly. Without the paramagnetic medium, the silicon particles will not experience large forces, and without magnetic forces, no self-assembly will take place. (3) Mechanical vibrations caused by a piezo transducer will be used as driving forces. These vibrations will allow the particles to explore the energy landscape and find an energy minimum. (4) For the binding force, two cases will be addressed. The first case involves hydrophilic particles, where only the magnetic force acts as a binding force. The second case covers hydrophobic particles, where both hydrophobic interaction between the particles and the magnetic force act as binding forces.

These experiments are a first step towards self-assembled three-dimensional crystals of microfabricated, anistropic

particles. In subsequent research, miniaturisation will be needed to move to self-assembled micro-structures, with as ultimate goal full three-dimensional microfabrication capabilites.

## II. Theory

Diamagnetic materials are repelled from magnetic fields [38], which makes diamagnetic materials perfect for magnetic levitation. The degree to which a material is diamagnetic is measured in the magnetic susceptibility $\chi$. For diamagnetic materials this is a negative number, for paramagnetic materials—materials attracted to magnetic fields—this is a positive number. Strongly diamagnetic materials, like pyrolitic graphite, are easy to levitate [28] in contrast to weakly diamagnetic materials. The challenge to levitate a weakly diamagnetic material, like silicon, can be overcome with a paramagnetic medium [39]. By surrounding the weakly diamagnetic material with a strongly paramagnetic medium, levitation can be achieved [31]. The paramagnetic medium is attracted to the magnets, pushing the diamagnetic material away: Magnetic levitation is achieved. The forces involved with diamagnetic levitation in a paramagnetic medium are twofold: On the one hand, there is a buoyant force, depending on the gravity, densities of the two materials, and volume of the diamagnetic particle. On the other hand, there is a magnetic force, which is dependant of the magnetic susceptibilities of the two materials, volume of the diamagnetic particle, and the applied magnetic field. Since both forces are a function of particle volume, the force per unit volume can be determined, see equation 1 [31].

$$\vec{F}/V = -(\rho_l - \rho_p)\,\vec{g} - \frac{(\chi_l - \chi_p)}{\mu_0}\left(\vec{B}\cdot\vec{\nabla}\right)\vec{B} \qquad (1)$$

Where $\vec{F}$ is the force on the particle, $V$ is its volume, $\rho$ is the density and $\chi$ the magnetic susceptibility of particle $p$ and liquid medium $l$. Vector $\vec{g}$ is the gravitational acceleration, $\mu_0$ the vacuum permeability and $\vec{B}$ the magnetic field. The density of silicon is $\rho_p = 2329\,\mathrm{kg/m^3}$ [40], the density of a 2 M $GdCl_3$ solution in water was measured to be $\rho_l = 1459\,\mathrm{kg/m^3}$. The magnetic susceptibility can be calculated for the $GdCl_3$ solution in water, see equation 2 [39].

$$\chi_l = 27.930 \cdot 10^{-3} \cdot 4\pi \cdot \mathrm{C} \qquad (2)$$

Where $C$ is the concenteration of $GdCl_3$ in water, in this work 2 M. The magnetic susceptibility of silicon is $\chi_p = -3.215 \cdot 10^{-3}$ [39].

In order to obtain a stable levitation point, two magnets can be placed close to eachother with similar poles facing [33]. To calculate the forces on a particle, the magnetic field needs to be determined. For the calculation of the magnetic field of a single magnet, the Biot-Savart equation was used, see equation 3 [38].

$$\vec{B}(\vec{r_1}) = \frac{\mu_0}{4\pi}\iiint \frac{\vec{j}(\vec{r_2})\times\vec{r_{12}}}{\vec{r_{12}}^{\,3}}dV_2 \qquad (3)$$

Where $\vec{B}$ is the magnetic field, $\mu_0$ is the permeability of free space, $\vec{r_{12}} = \vec{r_1} - \vec{r_2}$ is the full displacement vector, $\vec{j}$ is the current density in $V_2$, and $V_2$ is the volume of the magnet. To take advantage of the cylinder symmetry (in this work, cylindrical magnets were used), a cylindrical coordinate system is used. In the cylindrical coordinate system $r$, $\phi$ and $z$ are used as coordinate variables. The vectors $\vec{r_1}$ and $\vec{r_2}$ vectors take the form of $\vec{r_1} = [r_1, \phi_1, z_1]$ and $\vec{r_2} = [r_2, \phi_2, z_2]$. As indicated in equation 3, $\vec{r_2}$ is used for the integration volume, i.e. the magnet. The vector $\vec{r_1}$ is the location at which the magnetic field is calculated. Assuming the magnetisation is constant throughout the volume of the magnet, and using $\vec{j} = \nabla\times\vec{M}$ [38], then $\vec{j}$ is given by equation 4,

$$\vec{j} = M_z\,\delta(r_2 - R)\,\mathrm{u}(z_2)\,\mathrm{u}(L - z_2)\,\hat{\phi} \qquad (4)$$

where R is the radius of the magnet, L is the length of the magnet, $\delta$ is the dirac delta, u the step function and $\hat{\phi}$ is the unit vector of the $\phi$ direction. Note that $\phi_2$ can be taken as zero for our axisymmetrical system. The magnetisation of the magnets used in this work was calculated from a magnetic field measurement at the edge of the magnets, and is 1.25 T.

To obtain a two magnet model, the field of the second magnet is shifted by $z = L + h$ and superimposed on the field of the first magnet, where $h$ is the separation between the magnets.

To avoid elliptical integrals [41], implementation of equation 3 includes a discrete summation of the integral over $\phi$. All analytical calculations were performed using MATLAB[1]. The analytical model was verified with finite element method (FEM) simulations using COMSOL[2]; the FEM model agrees with the analytical calculations within 0.3 % in the region between the magnets.

The analytical calculations of the magnetic field were used to model the levitation height as in equation 1. In future work, these calculations can also be used to show energy reduction minimisation the self-assembly process.

## III. Experimental

In this section the details of the performed experiments are presented. First the production of the particles will be

[1] MATLAB R2013a, MathWorks, Nathick, US.
[2] COMSOL 4.3, COMSOL BV, Zoetermeer, The Netherlands.

discussed, followed by their chemical functionalisation. Finally, the set-up for self-assembly will be discussed.

### A. Particles

In the production of the particles, care was taken to make the faces of the cubes as smooth as possible. We feared that grooves on the surface of the particle could lead to an undesired preferred orientation between particles. We have chosen to use a dicing machine to create the particles. The cut surface was measured with a scanning electron microscope (SEM, FEI quanta 450) and an atomic force microscope(AFM, Dimension 3100) and the data was analysed with Gwyddion[3].

The cubic silicon particles were produced from a standard p-type double sided polished ⟨100⟩ 5-10 Ohmcm wafer. To ensure the produced particles are cubic, the thickness of the wafer was measured. The wafer was then sawed to create cubic particles with edges of the same length as the thickness of the wafer. A Loadpoint Micro Ace 3 dicing saw was used with a F1230 blade at 32000 rpm and a feed rate of 1 mm/sec. Residue of the dicing foil was removed by cleaning the particles with a 100 °C 1:4 piranha solution for ten minutes. The particles were then rinsed and stored in DI-water.

### B. Chemical functionalisation

Experiments to investigate the influence of hydrophobic interactions between the particles, required hydrophobic functionalisation of the particles. Hexamethyldisilazane (HMDS, BASF, VLSI Selectipur) was chosen for this goal because it is readily available and has been well characterised [42].

The particles were hydrophobically functionalised by allowing the surface silanol groups of the native oxide to react with HMDS, as shown in figure 1. The procedure to functionalise the particles with HMDS is based on previously published work [43, 44]. First, the particles were heated to remove water from the surface. Second, the particles were put in an erlenmeyer flask together with pure HMDS. The flask was closed with a stopper and was allowed to react, while being stirred, for two hours. The particles and HMDS were then poured through a funnel with a filter paper and rinsed with acetone (VWR Chemicals, Technical grade, 99 %) and isopropyl aclohol (Merck Millipore, for analysis, 99.8 %). Finally, the particles were allowed to dry in air. For the less hydrophobic variant, the particles were put in the funnel with filter paper directly after heating, rinsed with HMDS for one minute rather than two hours, and then finally rinsed with acetone and isopropyl alcohol. To measure the hydrophobicity of the particles, a non-sawed wafer received the same treatment. The contact angle of a droplet of water on the surface of the wafer was then measured with a Metrology Dataphysics OCA-20. The contact angle increased from 53° after 1 minute exposure to 93° after two hour exposure to HDMS.

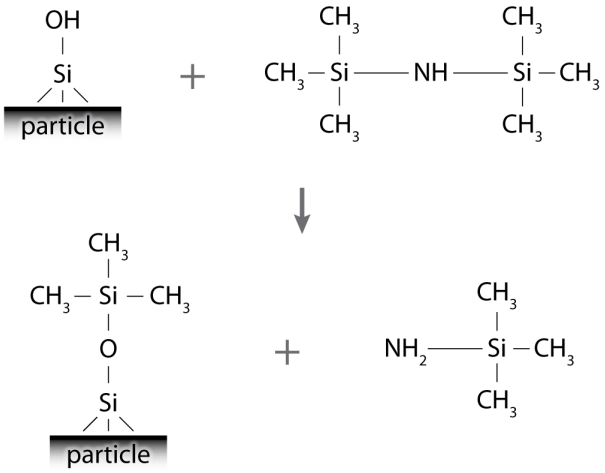


Figure 1: *Reaction equation for HMDS reacting with a silanol SiOH group of the native oxide on the surface of the silicon particles. When the HMDS (top right molecule) reacts with a silanol group on the surface of the particle, a trimethylsilyl $Si(CH_3)_3$ group replaces the hydrogen molecule on the surface of the particle. The hydrogen molecule bonds with the leftover amine NH group. The covalently bound trimethylsilyl group makes the surface of the particle apolar, causing hydrophobicity.*

### C. Self-assembly set-up

To combine all elements of self-assembly, a set-up was created from aluminum, see the schematic in figure 2. The set-up is capable of holding two magnets and a cuvette. Two holes are avaliable to observe the area between the magnets; the area where the self-assembly will take place. Two cameras were used to take photographs and record videos of the experiments. One Dino-lite pro usb microscope and one Nikon 1 J2 compact flash camera with a Macro-swistar 1:1.9 f=75 mm CMT lens and an 85 mm extention tube were used . Two NdFeB-magnets of 25 mm diameter and 35 mm length (a stack of five 7 mm magnets each) were used. The particles were inserted into a cuvette with a 2 M $GdCl_3$ solution in DI-water. The cuvette is pushed against a piezo actuator (FPA-0150E-S-0518-150-SS-1M3 FlexFrame PiezoActuator, dynamic, structures & materials, LLC), which supplies the driving forces for self-assembly. The cuvette is held in place by a spring. The piezo actuator is driven by an Agilent A33220A waveform generator connected to a 10x high voltage amplifier (SyLAB LM3325). The control parameters for

[3] Gwyddion 2.33, `http://gwyddion.net/`

the driving force—the piezo actuator—are the actuation frequency and amplitude, which are both configured on the waveform generator. The third control parameter is the time the particles are allowed to self-assemble.

To characterise the set-up and verify our model, the levitation height of one particle in the set-up was measured and compared against the analytical model. Non-magnetic, synthetic calipers (WIHA, Vernier Calipers #41103) were used to measure the levitation height. Characterisation of the driving force was performed by placing a microphone next to the set-up, and saving the fast fourier transform (FFT) of the recorded sound. The FFT was then summed to obtain a relative sound power.

In strong oscillatory fluid flows, particles can align in the nodes of standing waves [45, 46, 47, 48]. This phenomenon can be seen as a form of dynamic self-assembly, if the resulting structure is ordered [5]. For static self-assembly, actuation needs to be such that no strong fluid flows occur. In the results section, characterisation of the set-up is presented, and a suitable actuation frequency is chosen.

The quality of assembly was evaluated from photographs of the final agglomerate. Each observable particle was counted and its six faces were assessed for contact with other particles. This qualitative assesment led to five distinct categories: Good, displaced, unknown, bad, and no contact. Contacts with more than 95 % overlap between two faces are counted as good contacts. Contacts with a displacement, but no observable rotation between particles are counted as displaced contacts. A contact is counted as bad, if any kind of rotation can be observed. Faces of a particle that cannot be seen, are counted as unknown contacts. Finally, faces of a particle that do not touch another particle are counted as no contact. The good, displaced and bad contacts are counted as all observable contacts. It is assumed then that the unknown contacts adhere to the average of the observable contacts.

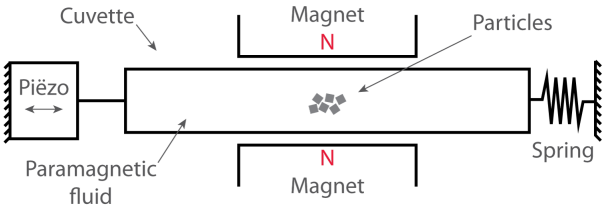


Figure 2: *Schematic of the set-up. A glass cuvette is inserted between two magnets, with similar poles facing. The cuvette is filled with paramagnetic fluid — 2M $GdCl_3$ in $H_2O$ solution— and silicon particles. The paramagnetic fluid is attracted to the magnets, pushing the silicon particles away from the magnet; the particles are levitated. With a piezo actuator and spring, vibrations can be applied to the cuvette. Through shaking, the particles can explore their energy landscape and find their energy minimum.*

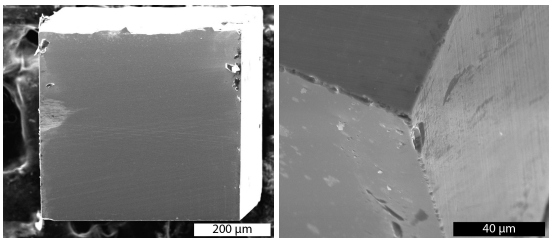


(a) (b)

Figure 3: *Two scanning electron micrographs of the particles. Left the full particle is shown, while on the right is a close-up of the corner to show the low rms surface roughness of 12.6 nm. The edges of the particle are 525 µm. These micrographs were made at a working distance of 11.8 mm, spot size 3 and an acceleration voltage of 15 kV.*

## IV. Results

In this section, the results will be presented. First, the characterisation of the set-up is presented, which includes three elements: Particle characterisation, particle levitation and piezo actuation. Second, the results of the self-assembly experiments will be presented, which likewise comprises three elements: levitated self-assembly, templated self-assembly and finally self-assembly with hydrophobically functionalised particles.

### A. *Characterisation of set-up*

The cut surface of the particles was observed with an SEM, see figure 3, and its roughness was measured using an AFM, see figure 4. Analysis of the results shows a disparity of 460 nm with a background root mean square (rms) roughness of 12.6 nm. Since no deep grooves are evident on the surface, we assume that there will be no preferred orientation with respect to another particle.

The levitation height of one particle was measured. The results show that the model agrees with the experimental results, see figure 5. The levitation height is plotted against magnet separation, and shows that the model agrees with the measurements.

The driving force was characterised, see figure 6. This is an indication on how much driving force the particles experience. In the 800 Hz to 1100 Hz range, the particles experience strong fluid flows, as evidenced by the structured arrays in figure 7.

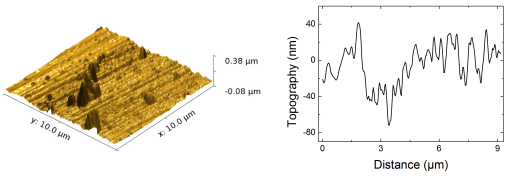


(a) (b)

Figure 4: *Measurements of the topography of the diced face of a particle. (a) Three-dimensional map of the scanned area. (b) Average of 10 lines perpendicular to the dicing marks. The disparity is 460 nm, with a background rms roughness of 12.6 nm.*

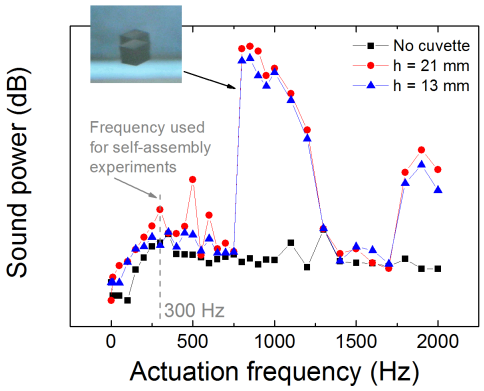


Figure 6: *Graph showing the power of the sound recorded by a microphone near the set-up at different driving frequencies at 130 $V_{pp}$. The FFT data for each driving frequency was summed to obtain a relative power. The 800 Hz to 1100 Hz frequency range corresponds to observations that indicate strong fluid flows.*

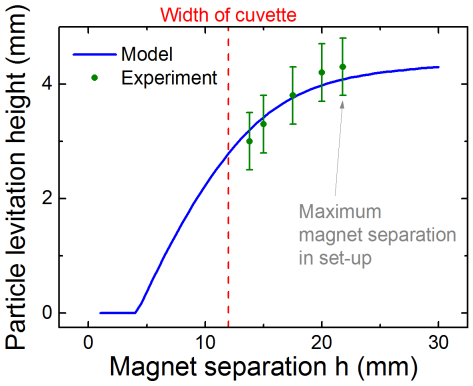


Figure 5: *Graph of the calculated and measured levitation heigh of the particles above the bottom magnet. The measured values are in good agreement with the model. The width of the cuvette is indicated by the dashed red line.*

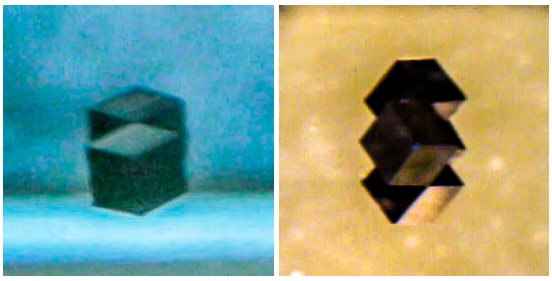

(a) (b)

Figure 7: *Photographs (contrast enhanced) taken of two (a) and four (b) particles during strong vibrations in the 800 Hz to 1100 Hz range. Strong fluid flows push the particles in an ordered array. This is a form of dynamic self-assembly [5]: An ordered array is formed while the system dissipates energy. When the oscillations are turned off, the array collapses. The edges of each particle are 525 µm.*

### B. Self-assembly

Different self-assembly experiments have been performed. A clear distinction is made between templated and levitated self-assembly. In templated self-assembly, the particles are introduced to a surface which puts some boundary conditions on the self-assembly process. Such a template can be a structured surface, but in this case the flat bottom of the cuvette was used as a template. This template reduces the degrees of freedom by three: two rotations and one translation. Under levitating conditions, self-assembly is performed without use of a template. The particles are levitated in the paramagnetic medium and allowed to self-assemble. First, levitated self-assembly of hydrophilic particles will be discussed. Second, templated self-assembly will be addressed. Finally, the influence of hydrophobic interactions between particles is presented.

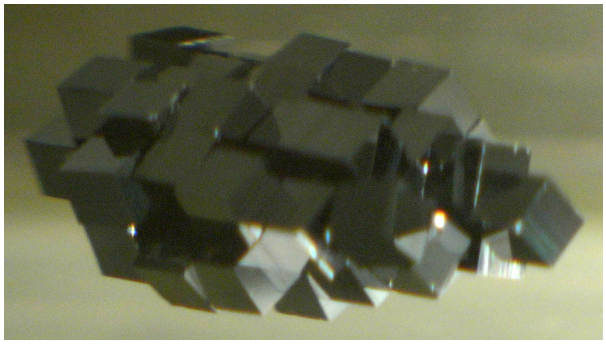

Figure 8: *Photograph (contrast enhanced) of three-dimensional self-assembly of levitated, hydrophilic, cubic silicon particles. Alignment between crystalline planes is suboptimal and alignment within crystalline planes is likewise suboptimal. The piezo was actuated at 300 Hz, 130 $V_{pp}$ for about 30 min to achieve this configuration. The edges of each particle are 525 µm.*

**Three-dimensional self-assembly of hydrophilic particles** Hydrophilic particles were inserted in the set-up and allowed to self-assemble for 30 min, at 300 Hz, 130 $V_{pp}$. The resulting agglomerate is shown in figure 8. Some good contacts can be observed, but long-range order is not directly evident. This result will later be compared to other self-assembly experiments.

**Templated self-assembly** Three different sets of templated self-assembly experiments were performed: Two-dimensional templated self-assembly, three-dimensional templated self-assembly, and seeded self-assembly. For seeded self-assembly, a plate the size of nine particles was introduced.

For two-dimensional templated self-assembly, particles were lowered onto the template and allowed to self-assemble at 300 Hz, 130 $V_{pp}$. Since the most substantial changes can be observed in the beginning of the process, photographs of the first 40 seconds are shown in figure 9, together with the assembly after 22 minutes. After 22 minutes a reconfiguration of the particles occured. We are still in the process to determine the energy development of the agglomerate. This series of photographs indicate that minimisation of the energy in the assembly takes place under influence of actuation by the piezo actuator, because the particles are moving closer together: A particle has the lowest energy at the central axis of the magnets.

A seed—a plate the size of 3x3x1 particles—was added to the two-dimensional templated self-assembly. Particles near the seed show good alignment, see figure 10. Especially in the two-dimensional case, the effect of the seed on the alignment between particles is evident. In the levitated self-assembly, particles near the seed show good alignment, but the effect decreases further away from the seed. This result shows the potential for seeded self-assembly: The seed locally increases the quality of the assembly.

Three-dimensional templated self-assembly was achieved by repeating the two-dimensional case, but with the particles levitating just enough to create a two-layer stack on the template. This three-dimensional self-assembly experiment resulted in an agglomerate as presented in figure 11. The result shows a large number of good contacts, and was compared to the levitated self-assembly results. In figure 12, a clear improvement of good contacts is evident: Templated self-assembly produces more than twice the amount of good contacts compared to levitated self-assembly.

**Hydrophobic particles** Finally, results for levitated self-assembly of hydrophobic particles are shown in figure 13. Compared to the hydrophilic case, this agglomerate shows a somewhat higher degree of alignment. Several well aligned planes can be seen, but there is room for improvement in alignment between these planes. The counted contacts are presented in figure 14. A clear increase of the sum of good and displaced contacts was observed for the 53° contact angle case. Since the other measurements show lesser alignment, there seems to be an optimal contact angle for self-assembly in the range between 0° to 93°.

## V. Discussion

As characterised by the sound power measurements in figure 6, in the range between 800 Hz to 1100 Hz strong fluid flows occur. This was however not exactly the same range for all experiments. Sometimes strong fluid flow

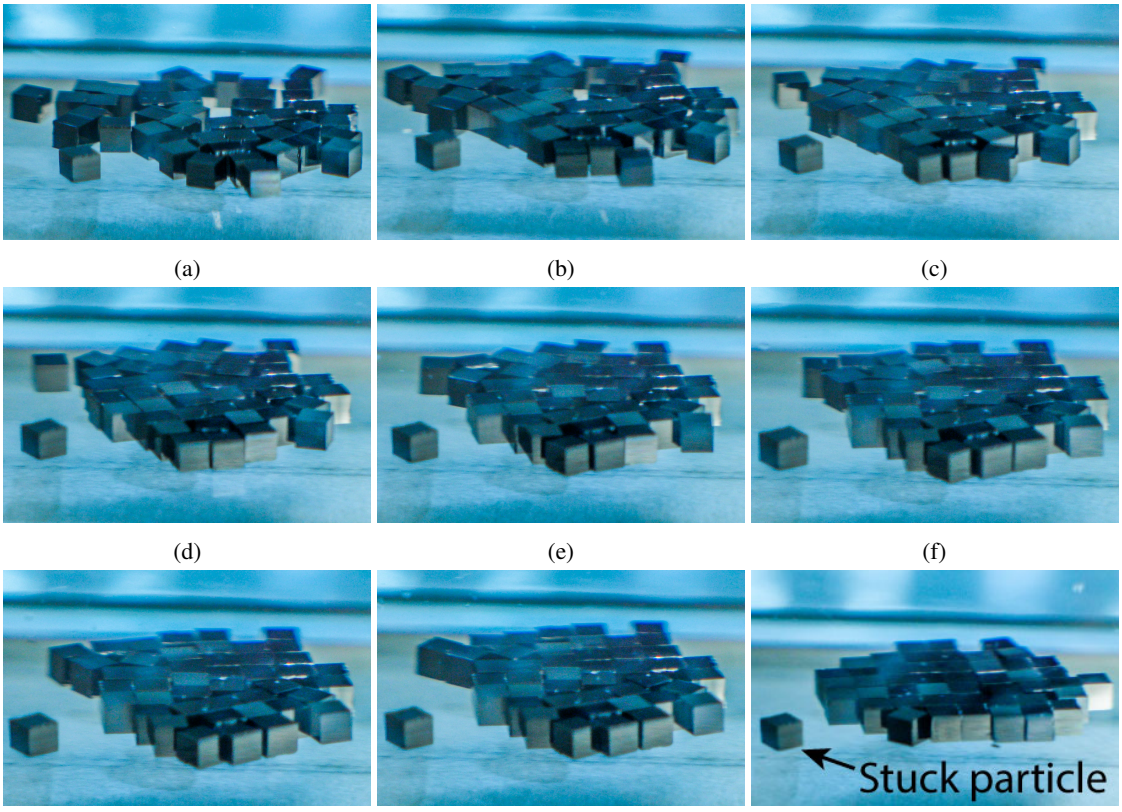


Figure 9: *Time lapse (contrast enhanced) of a templated two-dimensional self-assembly process. As time passes the particles move closer together to form an ordered array: energy minimisation occurs. Between each frame is 5 s, except for image (i) which shows the assembly after 22 min. The particles are resting on the bottom of the cuvette, which acts as a template for self-assembly. This structure was made with oscillations around the 300 Hz, with manually adjusted amplitude. Note that one particle was stuck to the cuvette, and is not moving. The edges of each particle are 525 µm.*

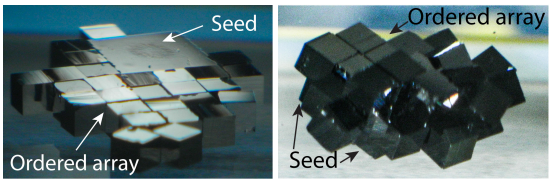


(a) (b)

Figure 10: *Two photographs (contrast enhanced) of self-assembly using a seed. (a) Image showing templated self-assembly on the bottom of the cuvette, with a seed. Good alignment of the particles can clearly be seen. (b) The seed and particles were levitated. A clear crystalline plane can be seen on the top left, where the particles are in direct contact with the seed below them. The edges of each particle are 525 µm.*

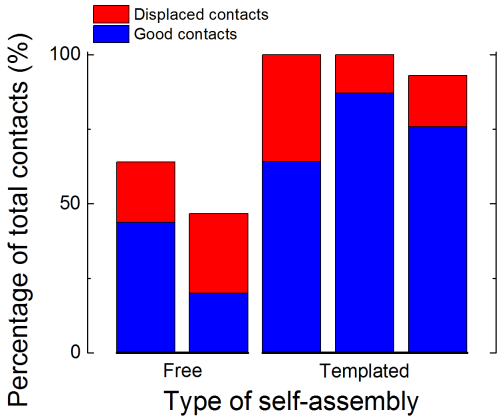


Figure 12: *Graph showing the number fully (blue) and fully plus displaced (red) aligned contact faces divided by the total of observed contact faces as a function of templating. These measurements were performed on photographs of three-dimensional self-assembled hydrophilic particles. A clear increase of alignment was observed for templated self-assembly: the amount of good contacts is more than twice as high for templated self-assembly than it is for untemplated self-assembly.*

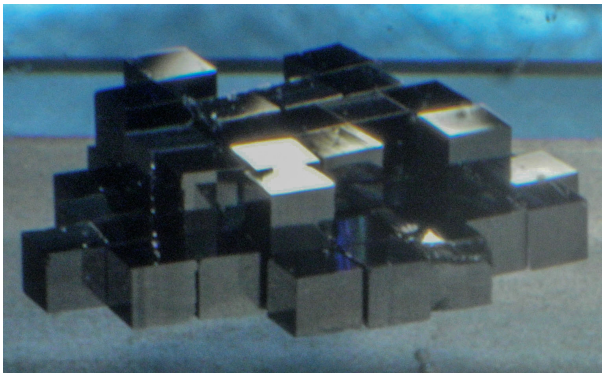

Figure 11: *This photograph (contrast enhanced) shows 54 particles in a self-assembled three-dimensional structure. The first layer of particles is resting on the bottom of the cuvette, which acts as a template for self-assembly. A high number of good contacts can be observed. The piezo ran at 300 Hz, 100 $V_{pp}$ for about 30 min to achieve this configuration. The edges of each particle are 525 µm.*

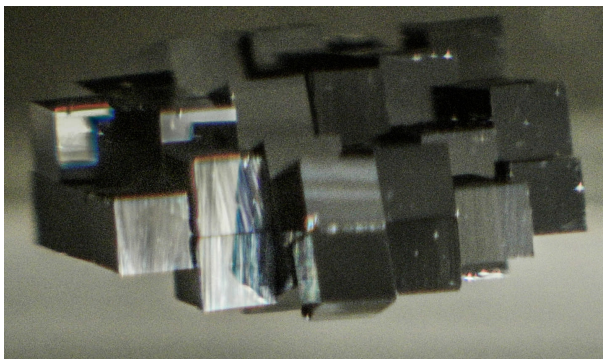

Figure 13: *Photograph (contrast enhanced) of a three-dimensional self-assembled, levitating agglomerate. The surface of the particles was functionalised with HMDS to induce hydrophobic interactions between the particles. Good alignment of particles can be seen for each plane, in contrast to the alignment between planes. The piezo ran at 300 Hz, 100 $V_{pp}$ for about 30 min to achieve this configuration. The edges of each particle are 525 µm.*

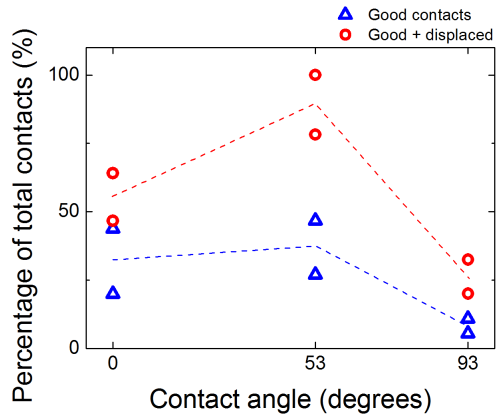


Figure 14: *Graph showing the number fully (blue) and fully plus displaced (red) aligned contact faces devided by the total of observed contact faces against the hydrophobicity of the particles, measured by the contact angle of a drop of water. A clear optimum can be seen for the hydrophobic particles with a 53° contact angle. The dashed lines act as a guide to the eye.*

occurred even at 300 Hz. We theorise that these fluid flows occur when the set-up is actuated near a resonant frequency, but that the exact frequency depends on two factors that differ per cuvette and experiment: (1) The air bubble volume and (2) the force with which the spring is loaded. Both values are not strictly controlled or measured, nor is it necessary to as long as care is taken not to induce strong fluid flows. A solution is either to lower the actuation amplitude, or change the actuation frequency. In this work the first option was chosen.

Looking at levitated self-assembly of both hydrophilic and hydrophobic particles, it seems that alignment between crystalline planes is a challenge. A first solution is the use of a template, as demonstrated in this work. However, we envision two other possible routes to overcome the challenge. On the one hand, the effect of hydrophobicity of the particles on the quality of the assembly can be further investigated. On the other hand, time could play an essential role in the alignment between crystalline planes, and longer self-assembly times can be explored.

From our data we conclude that templated self-assembly is superior to levitated self-assembly. We foresee that more investigation into templating can lead to better control over our self-assembly process. Modifying the template such that it leads to a different final configuration, can be another approach to obtain full three-dimensional micromachining capabilities. We propose two different approaches. A physical template can be introduced to change the final self-assembled configuration. Furthermore, the magnetic field could be adjusted to steer the particles differently and change the final self-assembled configuration.

Finally, we foresee that several parameters can be optimised. In this work we have kept the self-assembly conditions constant, where possible. That is, the actuation frequency, amplitude and time. In future work these parameters could be explored to find optimal conditions for each kind of particle and template. Such an extensive exploration is outside the scope of this study.

## VI. Conclusions

A self-assembly set-up was created and characterised. Cubic silicon particles with edges of 0.5 mm were produced with a dicing saw. On the cut surface, a disparity of 460 nm was measured with a background root mean square roughness of 12.6 nm (figure 4). These particles were placed in a paramagnetic medium between two magnets, with similar poles facing. The levitation height of silicon particles in a 2 M $GdCl_3$ solution in DI-water agrees with the presented model within $\pm$ 0.5 mm (figure 5). Driving forces for self-assembly were added by applying mechanical vibrations through the use of a piezo actuator. For static self-assembly, a workable vibration regime was found between 100 Hz to 700 Hz (figure 6).

From the templated two-dimensional self-assembly results, we conclude that by applying a mechanical vibration with a piezo actuator the energy of the assembly is reduced (figure 9). Applying mechanical vibrations using a piezo actuator is suitable to introduce driving forces.

Exposing the particles to a flat surface—a template—increases the percentage of good contacts by a factor two, with respect to self-assembly without a template (figure 12). In our experiments, applying a template is a suitable strategy to obtain good quality crystals.

The amount of good plus displaced contacts is a function of the hydrophobicity of the particles. An optimum was found for particles with a contact angle with water of 53°, at which the number of good plus displaced contacts was 30 % higher than for hydrophilic particles (figure 14). Adding hydrophobic functionalisation of the particles resulted in better quality crystals. However, hydrophobic interactions which are too strong are detrimental to the resulting structures, therefore care should be taken to functionalise the particles to a suitable degree of hydrophobicity.

To conclude: Self-assembly of cubic silicon particles was succesful, noting that aligning neighboring crystalline planes still provides a challenge. Templated self-assembly helpes in this respect by decreasing the number of degrees of freedom of the particles. Additionally, hydrophobic functionalisation of the particles to a

contact angle of 53° likewise increases the quatility of the assembled array. In future research we suggest a focus on moving to smaller scales, increasing the number of particles and exploring the benefits templated self-assembly can provide. The final goal is self-assembly of particles of arbitrary shape and size, and obtain full three-dimensional micromachining capabilities.

## VII. Acknowledgements

First of all, I would like to express my gratitude to everyone whom significantly contributed to this work: Léon Woldering, Laurens Alink, Garud Snoep, and Leon Abelmann. Likewise, I would like to thank Miko Elwenspoek and Jan Eijkel for the usefull discussions. In the same way, a lot of appreciation goes to Remco Sanders for his help building the set-up.

Thanks to my parents for supporting me and giving me the opportunity to study at the University of Twente. A big thank you goes to my brother, for always being there for me. Finally, I would like to thank my friends for all we have shared, in both happy and hard times.

## References

[1] R. Huber, J. Conrad, L. Schmitt, K. Hecker, J. Scheurer, and M. Weber, "Fabrication of multilevel silicon structures by anisotropic deep silicon etching," *Microelectronic Engineering*, vol. 67-68, pp. 410–416, 2003.

[2] Y. Taur, "CMOS design near the limit of scaling," *IBM Journal of Research and Development*, vol. 46, pp. 213–222, Mar. 2002.

[3] D. Park, K. Kim, and B. I. Ryu, "3-dimensional nano-CMOS transistors to overcome scaling limits," in *Proceedings of the 7th International Conference on Solid-State and Integrated Circuits Technology*, vol. 1, pp. 35–40, IEEE, 2004.

[4] G. M. Whitesides and B. Grzybowski, "Self-assembly at all scales," *Science*, vol. 295, no. March, pp. 2418–2421, 2002.

[5] J. A. Pelesko, *Self Assembly The Science of Things That Put Themselves Together*. Boca Raton: Chapman & Hall, 2007.

[6] L. Bragg and J. Nye, "A dynamical model of a crystal structure," *Proceedings of the Royal Society of London. Series A, Mathematical and Physical Sciences.*, vol. 190, no. 1023, pp. 474–481, 1947.

[7] L. Bragg and W. M. Lomer, "A Dynamical Model of a Crystal Structure. II," *Proceedings of the Royal Society A: Mathematical, Physical and Engineering Sciences*, vol. 196, pp. 171–181, Mar. 1949.

[8] D. H. Gracias, "Forming Electrical Networks in Three Dimensions by Self-Assembly," *Science*, vol. 289, pp. 1170–1172, Aug. 2000.

[9] M. Boncheva, R. Ferrigno, D. A. Bruzewicz, and G. M. Whitesides, "Plasticity in self-assembly: templating generates functionally different circuits from a single precursor.," *Angewandte Chemie (International ed. in English)*, vol. 42, pp. 3368–71, July 2003.

[10] M. Boncheva, S. A. Andreev, L. Mahadevan, A. Winkleman, D. R. Reichman, M. G. Prentiss, S. Whitesides, and G. M. Whitesides, "Magnetic self-assembly of three-dimensional surfaces from planar sheets," *Proceedings of the National Academy of Sciences of the United States of America*, vol. 102, pp. 3924–9, Mar. 2005.

[11] N. E. D. B. Bowden, M. Weck, I. S. Choi, and G. M. Whitesides, "Molecule-mimetic chemistry and mesoscale self-assembly.," *Accounts of chemical research*, vol. 34, pp. 231–8, Mar. 2001.

[12] L. A. Woldering, L. Abelmann, and M. C. Elwenspoek, "Predicted photonic band gaps in diamond-lattice crystals built from silicon truncated tetrahedrons," *Journal of Applied Physics*, vol. 110, no. 4, p. 043107, 2011.

[13] Y. Vlasov, X. Bo, J. Sturm, and D. Norris, "On-chip natural assembly of silicon photonic bandgap crystals," *Nature*, vol. 414, no. November, pp. 289–293, 2001.

[14] G. M. Whitesides and M. Boncheva, "Beyond molecules: self-assembly of mesoscopic and macroscopic components.," *Proceedings of the National Academy of Sciences of the United States of America*, vol. 99, pp. 4769–74, Apr. 2002.

[15] M. B. Cohn, K. F. Boehringer, J. M. Noworolski, A. Singh, C. G. Keller, K. A. Goldberg, and R. T. Howe, "Microassembly Technologies for MEMS," in *Proceedings of SPIE 3514, Micromachined Devices and Components IV* (M. E. Motamedi and H. P. Herzig, eds.), pp. 2–16, Sept. 1998.

[16] N. Bowden, A. Terfort, J. Carbeck, and G. M. Whitesides, "Self-Assembly of Mesoscale Objects into Ordered Two-Dimensional Arrays," *Science (New York, N.Y.)*, vol. 276, pp. 233–5, Apr. 1997.

[17] N. Bowden, I. S. Choi, B. A. Grzybowski, and G. M. Whitesides, "Mesoscale Self-Assembly of Hexagonal Plates Using Lateral Capillary Forces : Synthesis Using the Capillary Bond ," *Journal of the American Chemical Society*, vol. 121, no. 18, pp. 5373–5391, 1999.

[18] N. Bowden, S. R. J. Oliver, and G. M. Whitesides, "Mesoscale Self-Assembly: Capillary Bonds and Negative Menisci," *The Journal of Physical Chemistry B*, vol. 104, pp. 2714–2724, Mar. 2000.

[19] R. J. Knuesel and H. O. Jacobs, "Self-assembly of microscopic chiplets at a liquid–liquid-solid interface forming a flexible segmented monocrystalline solar cell," 2009.

[20] U. Srinivasan, D. Liepmann, and R. Howe, "Microstructure to substrate self-assembly using capillary forces," *Journal of Microelectromechanical Systems*, vol. 10, pp. 17–24, Mar. 2001.

[21] U. Srinivasan, M. A. Helmbrecht, C. Rembe, R. S. Muller, and R. T. Howe, "Fluidic Self-Assembly of Micromirrors Onto Microactuators Using Capillary Forces," *IEEE Journal on selected topics in quantum electronics*, vol. 8, no. 1, pp. 4–11, 2002.

[22] T. Fukushima, E. Iwata, T. Konno, J. Bea, K. Lee, T. Tanaka, and M. Koyanagi, "Surface tension driven chip self-assembly with load-free hydrogen fluoride-assisted direct bonding at room temperature for three-dimensional integrated circuits," *Applied Physics Letters*, vol. 96, no. 15, p. 154105, 2010.

[23] G. E. Fernandes, D. J. Beltran-Villegas, and M. A. Bevan, "Spatially controlled reversible colloidal self-assembly.," *The Journal of Chemical Physics*, vol. 131, p. 134705, Oct. 2009.

[24] M. Rycenga, J. M. McLellan, and Y. Xia, "Controlling the Assembly of Silver Nanocubes through Selective Functionalization of Their Faces," *Advanced Materials*, vol. 20, pp. 2416–2420, June 2008.

[25] T. D. Clark, J. Tien, D. C. Duffy, K. E. Paul, and G. M. Whitesides, "Self-assembly of 10-microm-sized objects into ordered three-dimensional arrays.," *Journal of the American Chemical Society*, vol. 123, pp. 7677–82, Aug. 2001.

[26] H. Onoe, K. Matsumoto, and I. Shimoyama, "Three-dimensional

sequential self-assembly of microscale objects.," *Small (Weinheim an der Bergstrasse, Germany)*, vol. 3, pp. 1383–9, Aug. 2007.

[27] F. Ilievski, K. A. Mirica, A. K. Ellerbee, and G. M. Whitesides, "Templated self-assembly in three dimensions using magnetic levitation," *Soft Matter*, vol. 7, no. 19, p. 9113, 2011.

[28] R. Pelrine, "Diamagnetic Levitation," *American Scientist*, vol. 92, no. 5, pp. 428–435, 2004.

[29] T. Kimura, S. Mamada, and M. Yamato, "Separation of solid polymers by magneto-Archimedes levitation," *Chemistry Letters*, pp. 1294–1295, 2000.

[30] Y. Ikezoe, N. Hirota, J. Nakagawa, and K. Kitazawa, "Making water levitate," *Nature*, vol. 393, no. June, pp. 749–750, 1998.

[31] A. Winkleman, R. Perez-Castillejos, K. L. Gudiksen, S. T. Phillips, M. Prentiss, and G. M. Whitesides, "Density-based diamagnetic separation: devices for detecting binding events and for collecting unlabeled diamagnetic particles in paramagnetic solutions," *Analytical chemistry*, vol. 79, pp. 6542–50, Sept. 2007.

[32] K. Yokoyama, N. Hirota, and M. Iwasaka, "Separation of Collagen by Magneto-Archimedes Levitation," *IEEE Transactions on Applied Superconductivity*, vol. 17, pp. 2181–2184, June 2007.

[33] K. A. Mirica, S. T. Phillips, S. S. Shevkoplyas, and G. M. Whitesides, "Using magnetic levitation to distinguish atomic-level differences in chemical composition of polymers, and to monitor chemical reactions on solid supports.," *Journal of the American Chemical Society*, vol. 130, pp. 17678–80, Dec. 2008.

[34] K. A. Mirica, S. S. Shevkoplyas, S. T. Phillips, M. Gupta, and G. M. Whitesides, "Measuring densities of solids and liquids using magnetic levitation: Fundamentals.," *Journal of the American Chemical Society*, vol. 131, pp. 10049–58, July 2009.

[35] K. A. Mirica, F. Ilievski, A. K. Ellerbee, S. S. Shevkoplyas, and G. M. Whitesides, "Using magnetic levitation for three dimensional self-assembly.," *Advanced materials (Deerfield Beach, Fla.)*, vol. 23, pp. 4134–40, Sept. 2011.

[36] E. J. W. Berenschot, H. V. Jansen, and N. R. Tas, "Fabrication of 3D fractal structures using nanoscale anisotropic etching of single crystalline silicon," *Journal of Micromechanics and Microengineering*, vol. 23, p. 055024, May 2013.

[37] I. Lyuksyutov and A. Lyuksyutova, "Trapping microparticles with strongly inhomogeneous magnetic fields," *Modern Physics Letters B*, vol. 17, no. 17, pp. 935–940, 2003.

[38] R. P. Feynman, R. B. Leighton, and M. Sands, *The Feynmann Lectures on Physics, Volume II*. Pearson Addison Wesley, definitive ed., 1964.

[39] W. M. Haynes, "Magnetic susceptibility of the elements and inorganic compounds," in *CRC handbook of chemistry and physics, 94th Edition*, vol. 94, pp. 4.131–4.136, 2013.

[40] W. M. Haynes, "Physical Constants of Inorganic Compounds List of Abbreviations," in *CRC handbook of chemistry and physics, 94th Edition*, pp. 4.43–4.101, 2013.

[41] R. Ravaud, G. Lemarquand, S. Babic, V. Lemarquand, and C. Akyel, "Cylindrical Magnets and Coils: Fields, Forces, and Inductances," *IEEE Transactions on Magnetics*, vol. 46, pp. 3585–3590, Sept. 2010.

[42] M. Hair and W. Hertl, "Reaction of hexamethyldisilazane with silica," *The Journal of Physical Chemistry*, vol. 76, no. 14, pp. 3–7, 1971.

[43] A. Awomolo, L. Jiang, J. Zhang, G. Jursich, and C. Takoudis, "Dielectric Materials in Organic Thin Film Transistors," *Journal of Undergraduate Research*, vol. 1, no. 47, pp. 47–51, 2007.

[44] J. Lu, H. Takagi, and R. Maeda, "Chip to wafer temporary bonding with self-alignment by patterned FDTS layer for size-free MEMS integration," in *2011 IEEE SENSORS Proceedings*, pp. 1121–1124, IEEE, Oct. 2011.

[45] D. Klotsa, M. Swift, R. Bowley, and P. King, "Chain formation of spheres in oscillatory fluid flows," *Physical Review E*, vol. 79, p. 021302, Feb. 2009.

[46] D. V. Lyubimov, A. Y. Baydin, and T. P. Lyubimova, "Particle Dynamics in a Fluid Under High Frequency Vibrations of Linear Polarization," *Microgravity Science and Technology*, vol. 25, pp. 121–126, Jan. 2013.

[47] D. V. Lyubimov, A. A. Cherepanov, T. P. Lyubimova, and B. Roux, "Interface orienting by vibration," *Comptes Rendus de l'Académie des Sciences - Série IIB*, vol. 325, no. 1, pp. 391–396, 1997.

[48] H. A. Pacheco-Martinez, L. Liao, R. J. A. Hill, M. R. Swift, and R. M. Bowley, "Spontaneous Orbiting of Two Spheres Levitated in a Vibrated Liquid," *Physical Review Letters*, vol. 110, p. 154501, Apr. 2013.